Photoluminescence from defects in GaN

M. A. Reshchikov*^a
^a Department of Physics, Virginia Commonwealth University, 701 West Grace St., Richmond, VA,
USA 23220-4116

ABSTRACT

We present the most recent results of photoluminescence (PL) studies, classification of defects in GaN and their properties. In particular, the yellow luminescence band (labeled YL1) with a maximum at 2.17 eV in undoped GaN grown by most common techniques is unambiguously attributed to the isolated C_N acceptor. From the zero-phonon line (ZPL) at 2.59 eV, the -/0 level of this acceptor is found at 0.916 eV above the valence band. The PL also reveals the 0/+ level of the C_N at 0.33 eV above the valence band, which is responsible for the blue band (BLc), with the ZPL at 3.17 eV. Another yellow band (YL2) with a maximum at 2.3 eV, observed only in GaN grown by the ammonothermal method, is attributed to the V_{Ga} 3H complex. The nitrogen vacancy (V_N) causes the green luminescence (GL2) band. The V_N also forms complexes with acceptors such as Mg, Be, and Ca. These complexes are responsible for the red luminescence bands (the RL2 family) in high-resistivity GaN. The results from PL studies are compared with theoretical predictions. Uncertainties in the parameters of defects are discussed.

Keywords: Photoluminescence, GaN, point defects, zero-phonon line, yellow band

1. INTRODUCTION

Understanding and identifying point defects in GaN is essential for increasing the efficiency of GaN-based light-emitting and high-power devices. Identifying point defects in GaN and finding their parameters is also critical for developing modern theoretical approaches. Photoluminescence (PL) is one of the most powerful tools to determine the parameters of point defects with high precision. Significant progress in the understanding of PL from defects in GaN has been achieved since our previous review. Improvements in crystal quality and reduction of structural and point defects led to the discovery of zero-phonon lines (ZPL) for PL bands from several defects in GaN. The charge transition levels can be found from the ZPL with high accuracy and compared with predictions of first-principles calculations. In particular, the omnipresent yellow luminescence (YL) band in undoped GaN is unambiguously assigned to the isolated C_N acceptor.^{2,3} The ZPL at 2.59 eV and the characteristic phonon-related fine structure have been found, which now serve as fingerprints of the YL band (named YL1).⁴ In addition to the -/0 transition level, the C_N defect has a donor-like 0/+ level at 0.33 eV above the valence band maximum (VBM). Electron transitions via this level are responsible for the blue luminescence (BL_C) band with a maximum at 2.85 eV and ZPL at 3.17 eV.^{5,6} A new mechanism of PL quenching has been discovered - abrupt and tunable quenching of PL.7 This is the primary mechanism for semi-insulating GaN (undoped and doped with acceptors).8 It is also responsible for a superlinear increase of PL with excitation intensity.9 Strong electric fields in semi-insulating GaN can cause significant shifts of PL bands with excitation intensity and affect the thermal quenching of PL. 10,11 Photoinduced dissociation of defect complexes, such as C_NH_i, has been explained. 12 Significant progress in the understanding of point defects in GaN has also been achieved in first-principles calculations. 13,14 In this Review, we focus on new findings about PL from defects in GaN.

^{*}mreshchi@vcu.edu; phone 1 804 828-1613; fax 1 804 828-7073; physics.vcu.edu

2. METHODS

2.1 Photoluminescence experiment

Details of the PL experiment can be found in Ref. 8. The two main techniques in the PL experiment are steady-state PL (SSPL) and time-resolved PL (TRPL).^{5,15} In this review and our publications since 2018, the as-measured PL spectra are not only corrected for the measurement system's spectral response but additionally multiplied by λ^3 , where λ is the light wavelength, to present the PL spectra in units proportional to the number of emitted photons as a function of photon energy.⁵ Note that such corrections may change the shapes, relative contributions, and positions of broad PL bands.⁸ The light excitation intensity or photon flux, P, can be found from the excitation power density, P_{exc} , by converting Watts into the number of photons with energy hv_{exc} (for the He-Cd laser, $P_{exc} = 1 \text{ W/cm}^2$ converts to $P \approx 1.6 \times 10^{18} \text{ cm}^2 \text{s}^{-1}$).¹⁶ The laser light intensity inside GaN decreases as $\exp(-\alpha x)$, where α is the absorption coefficient ($\alpha \approx 1.2 \times 10^5 \text{ cm}^{-1}$ for GaN at $\hbar \omega = 3.8 \text{ eV}$),¹⁷ and α is the distance from the surface into the sample. In the simplest approximation, the electron-hole pair generation rate α (cm⁻³s⁻¹) can be determined from α as α as α as α as found by comparing the intensity after integrating over the PL band with that from calibrated GaN samples.^{7,8,18}

2.2 Analysis of photoluminescence data

Parameters of point defects responsible for PL bands can be found from analysis of SSPL and TRPL data obtained in a wide range of excitation intensities and temperatures. ^{1,8} These include the electron- and hole-capture coefficients (C_n and C_p , respectively) and thermodynamic charge transition level associated with the ZPL of PL. For n-type GaN with the concentration of free electrons n, electron transitions from the conduction band to the defect level occur with a characteristic time τ_0 (the PL lifetime) that can be found from TRPL measurements:

$$\tau_0 = \left(nC_n\right)^{-1}.\tag{1}$$

With increasing temperature T, the experimentally-measured PL lifetime varies as

$$\tau(T) = \frac{\tau_0}{1 + C \exp\left(-E_4 / kT\right)},\tag{2}$$

i.e., it decreases exponentially above a critical temperature T_0 , which can be found from the relation

$$E_A = kT_0 \ln C. (3)$$

The PL intensity, I^{PL} , has a similar temperature dependence:

$$I^{PL}(T) = \frac{I_0^{PL}}{1 + C \exp(-E_A / kT)}.$$
 (4)

In both cases, $C = (1 - \eta_0) \tau_0 C_p N_v g^{-1}$, where η_0 and τ_0 are the PL IQE and PL lifetime, respectively, at $T < T_0$; N_v is the effective density of states in the valence band (we assume $N_v = N_v T^{3/2}$ with $N_v' = 3.15 \times 10^{15}$ cm⁻³K^{-3/2} for GaN); k is Boltzmann's constant; and g is the degeneracy of the defect level (assumed g = 2). The E_A in these expressions is the activation energy (the defect ionization energy), which is equal to the distance from the defect level to the valence band maximum (VBM) plus a potential barrier for the hole capture if any. The exponential decrease of PL intensity is called PL quenching, and it is caused by the emission of holes from the defect to the valence band with the characteristic time $\tau_{therm} = \tau_0 C^{-1} \exp(E_A/kT)$. The quenching caused by the thermal emission of minority carriers and their redistribution between different recombination channels (the Schön-Klasens mechanism)¹⁹ is typical for n-type GaN. From the fit of experimental data with Eqs. (2) and (4) parameters E_A and C_p can be determined.

For semi-insulating (SI) GaN, the abrupt and tunable quenching mechanism is typical.⁷ The $I^{PL}(T)$ dependence can be formally described with Eq. (4), yet the parameters C and E_A in this case do not have physical meaning. The parameter E_A may significantly exceed the ionization energy (the abrupt quenching), and T_0 increases with P_{exc} (tunable quenching). For such samples, C = B/G, and the defect ionization energy can be found from the following expression ⁷

$$E_A = kT_0 \ln(B/G). \tag{5}$$

Here, $B = (\eta_0^{-1} - 1)(N_A - N_D)C_p N_v g^{-1}$, N_A and N_D are the concentrations of acceptors and shallow donors. The abrupt and tunable quenching is reminiscent of a phase transition: at $T < T_0$, the recombination efficiency is dictated by defects that

capture holes more efficiently, whereas at $T > T_0$, the dominant recombination channels are deep donors that capture electrons faster.

The shape of a defect-related PL band can be fitted with the following expression obtained in a one-dimensional configuration coordinate model 20

$$I^{PL}(\hbar) \qquad \hbar \qquad \left[-2S_e \left(\sqrt{\frac{E_0^* - \hbar}{d_{FC}^*}} \right)^2 \right]. \tag{6}$$

Here, S_e is the Huang-Rhys factor in the excited state of the defect, $d_{FC}{}^g = E_0{}^* - \hbar \omega_{\text{max}}$ is the Franck-Condon shift in the ground state, $E_0{}^* = E_0 + 0.5\hbar \Omega_e$, $E_0{}^*$ is the ZPL energy, $\hbar \Omega_e{}^*$ is the energy of the effective phonon mode in the excited state, $\hbar \omega$ and $\hbar \omega_{\text{max}}$ are the photon energy and position of the PL band maximum, respectively. The Δ is a minor shift of the PL band maximum due to sample-dependent reasons such as in-plane biaxial strain in thin GaN layers grown on sapphire substrates or local electric fields.

The concentrations of defects N can be found from the dependence of PL intensity on the excitation photon flux 21

$$\frac{I^{PL}(P)}{I_0^{PL}} = \frac{\eta(P)}{\eta_0} = \frac{P^{cr}}{P} \ln\left(1 + \frac{P}{P^{cr}}\right)$$
 (7)

with $P^{cr} = N(\eta_0 \alpha \tau_0)^{-1}$. Here, η_0 and I_0^{PL} are the IQE and PL intensity, respectively, in the limit of low excitation intensity.

3. RESULTS

Parameters of major defect-related PL bands in GaN are given in Table 1. Most of these PL bands are identified. In unintentionally doped GaN, the PL bands appear due to unavoidable contamination during GaN growth. Note that the concentration of related defects may be low, and particular PL bands are intense because the defects capture minority carriers (holes in *n*-type) very efficiently. The contamination depends on the growth technique. In particular, GaN grown by metalorganic chemical vapor deposition (MOCVD) contains carbon impurities, and the C_N-related YL1 band is usually strong.

Table 1. Parameters of defect-related PL bands in GaN.

PL band name	Attribution	ZPL	$\hbar\omega_{\mathrm{max}}$	E_A	C_p	C_n	τ	S_e	E_0^*
		(eV)	(eV)	(eV)	(cm^3/s)	(cm^3/s)	(µs)		(eV)
UVL _{Be}	Be _{Ga} (-/0)	3.38	3.38	0.113	~10-6	1×10 ⁻¹¹	10 ^a	0.2 ± 0.03	-
UVL, UVL _{Mg}	$Mg_{Ga}(-/0)$	3.28	3.28	0.224	1×10^{-6}	3.2×10 ⁻¹²	30 ^a	0.4 ± 0.05	-
BL1, BL _{Zn}	$Zn_{Ga}(-/0)$	3.10	2.86	0.400	5×10 ⁻⁷	6.8×10^{-13}	150a	3.2 (2.8-3.6)	3.14 ± 0.02
BL2	$C_N H_i (0/+)$	3.33	3.00	0.15	4.5×10 ⁻⁸	-	0.30^{b}	4.6 (4-5)	3.38 ± 0.02
BL_C	$C_{N}(0/+)$	3.17	2.85	0.33	~10-10	~10-9	$0.001^{\rm b}$	3.5 (2.5-4)	3.20 ± 0.03
BL3	"RY3" (0/+)	3.01	2.80	0.46	~10-9	-	$0.001^{\rm b}$	2.0 (1.6-2.5)	3.07 ± 0.03
BLcd	Cd _{Ga} (-/0)	2.96	2.70	0.55	-	-	-	4.0 (3.5-4.5)	3.00 ± 0.02
GL1	? (0/+)	-	2.35	~0.5	3.7×10^{-8}	-	1°	10.3 (7-14)	2.97 ± 0.10
GL2	$V_N (+/2+)$	-	2.33	~0.7	-	-	250^{b}	13.5 (10-18)	2.70 ± 0.05
AL, GL _{Ca}	$Ca_{Ga}(-/0)$	-	2.50	0.50	6×10^{-7}	9×10^{-14}	1100a	8.5 (7-10)	3.00 ± 0.03
$YL1, YL_C$	$C_{N}(-/0)$	2.59	2.17	0.916	3.7×10 ⁻⁷	1.1×10^{-13}	900^{a}	7.8 (6.5-9)	2.67 ± 0.03
YL2	$V_{Ga}3H_{i}(0/+)$	-	2.3	~0.6	-	-	-	7 (5-9)	2.87 ± 0.1
YL3	"RY3" (-/0)	2.38	2.07	1.130	~10-7	2×10^{-13}	500^{a}	6.2 (5-7.5)	2.41 ± 0.03
YL_{Be}	$Be_{Ga}(-/0)$	-	2.15	0.3	4×10 ⁻⁷	1×10^{-13}	1000^{a}	23 (18-28)	3.2 ± 0.1
RL1	C1? (-/0)	-	1.73	~1.2	2.9×10 ⁻⁷	4.3×10 ⁻¹⁴	2200a	14 (9-22)	2.4 ± 0.15
RL2	$V_{NA}(0/+)$	-	1.72	~0.9	-	-	110^{b}	20 (10-30)	2.45 ± 0.15
RL_{Mg}	$V_N Mg_{Ga} (0/+)$	-	1.73				1.4 ^b	12.5 (10-16)	2.3 ± 0.1
RL_{Be}	$V_N Be_{Ga} (0/+)$	-	1.77	~0.8	-	-	3 ^b	15 (7-27)	2.6 ± 0.2
RL_{Ca}	$V_N Ca_{Ga} (0/+)$	-	1.82	~1.1	-	-	2000^{b}	12 (6-18)	2.2 ± 0.1
RL3	"RY3" (-/0)	-	1.77	~2.6	~10-5	-	0.010^{b}	-	-

^a For $n = 10^{16}$ cm⁻³

^b Internal transition at T = 18 K

^c Internal transition at T = 100 K

The RL3, YL3, and BL3 bands are three emission bands from a single defect (called the RY3 center) and observed in GaN grown by hydride vapor phase epitaxy (HVPE). Two other PL bands in undoped GaN produced by HVPE are the RL1 and GL1 bands. GaN samples grown by molecular beam epitaxy (MBE) at relatively low temperatures are often contaminated by Ca and exhibit a strong GL_{Ca} band. The YL2 band is observed only in GaN grown by the ammonothermal method, where high concentrations of gallium vacancies (V_{Ga}), oxygen, and hydrogen are unavoidable.

The appearance of PL bands also depends on conductivity type. In conductive n-type GaN, the capture of photogenerated holes dictates the electron-hole recombination efficiency, and acceptors usually contribute to PL spectra. In semi-insulating GaN, the efficiency of electron capture may dictate the PL intensities, and donor-related PL bands appear. For example, the nitrogen vacancy (V_N) is a deep donor with the \pm 2+ transition level at about 0.4-0.7 eV above the VBM. The V_N is responsible for the green (GL2) band, with a maximum at 2.33 eV.

3.1 Acceptors

In n-type GaN, PL from only acceptors is usually observed because negatively charged acceptors attract holes and have large hole-capture coefficients, C_p (Table 1). Even in undoped GaN, PL related to the Mg_{Ga}, Zn_{Ga}, and C_N acceptors (the UVL_{Mg}, BL1, and YL1 bands, respectively) may have quantum efficiency close to unity due to contamination with impurities at levels close to or below the detection limit of secondary-ion mass-spectrometry (SIMS), typically around 10¹⁶ cm⁻³. The RL1 band is the dominant PL band in undoped GaN grown by HVPE and presumably caused by Cl. Figure 1 shows the shapes of these PL bands at a low temperature. In high-quality GaN crystals, the ZPL of the UVL_{Mo}, BL1, YL1, and YL3 bands can be observed (Table 1). For all these acceptors, PL at T < 50 K is caused by electron transitions from shallow donors (O_N or Si_{Ga}) to the -/0 transition level, the so-called donor-acceptor pair (DAP) transitions. This PL (including ZPL) shifts to higher photon energies by about 7 meV as the $P_{\rm exc}$ increases from ~10⁻⁴ to 1 W/cm². At T > 50 K, the DAP transitions are replaced with transitions from the conduction band to the -/0 level, the eA transitions. The eA components of PL (including the ZPL, phonon replicas, and broad envelope) emerge at higher photon energies (~20 meV above the DAP components), and the PL band shape usually does not change much up to a critical temperature T_0 . At $T > T_0$, the PL intensity decreases exponentially, and the temperature dependence can be fitted with Eq. (4). With known τ_0 (found from TRPL experiments) and η_0 (usually estimated from a comparison of PL intensity with that from calibrated samples), the C_p and E_A can be found from the fit with Eq. (4). Note that sometimes the obtained parameter E_A is smaller than the distance from the -/0 transition level to the VBM due to diagonal transitions in crystals with a high concentration of defects.

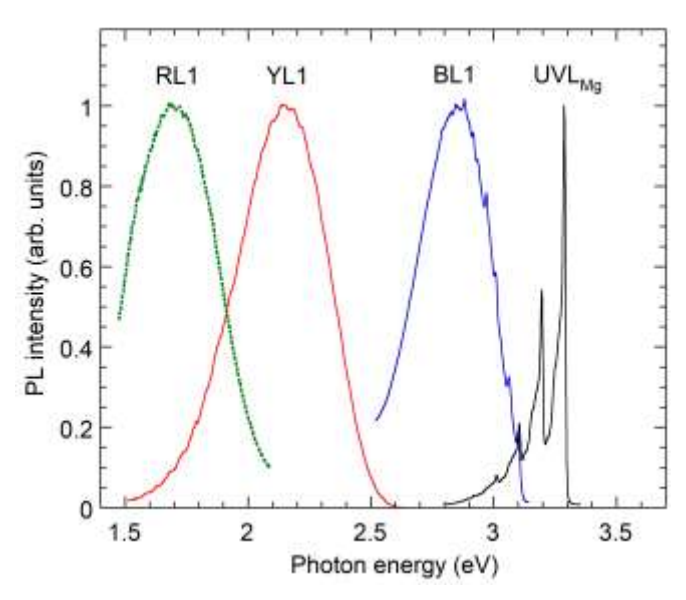


Figure 1. PL spectra from major acceptors in undoped GaN at T = 18 K. The UVL_{Mg}, BL1, and YL1 bands are related to the MgGa, ZnGa, and C_N acceptors, respectively.

In TRPL, the nonexponential decay of PL at low temperatures is explained by the DAP nature of transitions.²⁵ At T > 50 K, eA transitions gradually replace the DAP transitions, and PL decay after a laser pulse becomes more and more exponential. The characteristic time of PL decay, τ_0 , is inversely proportional to the concentration of free electrons, see Eq. (1). At intermediate temperatures (when the DAP and eA contributions are comparable) τ_0 can be defined as the time at which the $I^{PL}(t)t$ dependence has a maximum.²⁶

3.2 Donors

PL from donors is rarely observed in n-type GaN. Among the reasons are low formation energy of donors and low C_p resulting in inefficient capture of photogenerated holes. The PL from donors in GaN is usually caused by internal transitions: from an excited state close to the conduction band to the ground state.⁸ In this case, the PL decay is exponential even at very low temperatures and independent of n. A well-studied case is the C_NH_i complex which has a 0/+ level at 0.15 eV above the VBM. The V_N is a deep donor with the +/2+ transition level at ~ 0.5 eV above the VBM and an excited state close to the conduction band. The internal transitions in this defect are responsible for the GL2 band with a maximum at 2.33 eV. The GL2 band is observed only in semi-insulating GaN. First, an electron is captured by the excited state; then, a hole is captured at the +/2+ level. In conductive n-type GaN, the GL2 band is not observed even if the nitrogen vacancies are abundant because the defects are neutral. In conductive p-type GaN, the GL2 band may not be observed because the defects are in the 3+ state. The V_N forms complexes with acceptors in GaN. The resulting V_N A complexes are deep donors responsible for red PL bands. In particular, Ca_{Ga} , Mg_{Ga} , and Be_{Ga} form complexes with V_N .^{8,27,28} The RL2 band in undoped GaN is also presumably caused by the V_N A complex, yet the origin of the acceptor is unknown. Figure 2 shows PL spectra from typical donors in GaN.

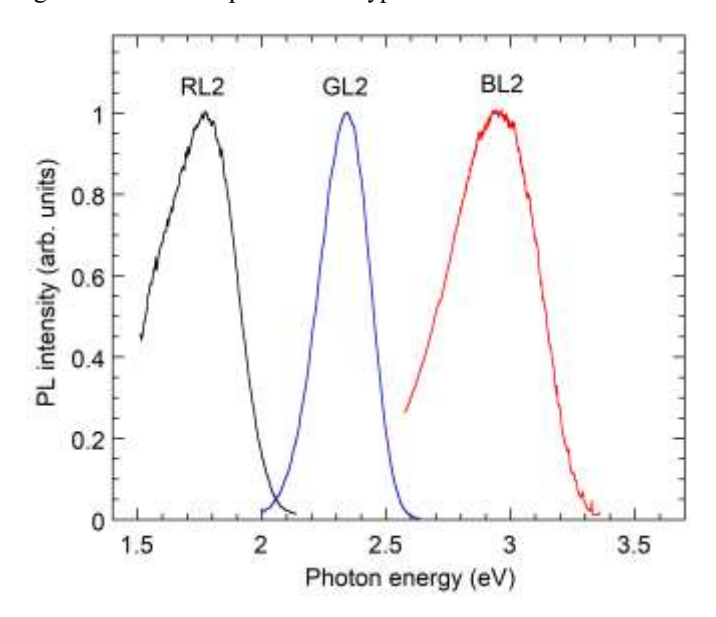


Figure 2. PL spectra from donors in undoped GaN at T = 18 K. The RL2 and GL2 bands are related to the V_N , and the BL2 band is caused by the C_NH_i complex.

In GaN, defects often have more than one charge transition level in the gap. At high excitation intensity, the acceptors can be saturated with holes, and new holes will be captured by the 0/+ level. For example, a saturation of the YL1 band in n-type GaN leads to the emergence of the BL $_{\rm C}$ band. The BL $_{\rm C}$ band with a maximum at 2.85 eV and ZPL at 3.17 eV is caused by electron transitions from an excited state near the conduction band to the donor-like state of the $C_{\rm N}$ located at 0.33 eV above the VBM. Similarly, the BL3 band is the secondary PL band of the RY3 acceptor, and the GL1 band is the secondary PL band of an unknown acceptor in HVPE GaN (predicted in the infrared region).

Complexes containing the V_{Ga} , such as $V_{Ga}3H$, $V_{Ga}2O_NH$, $V_{Ga}O_N2H$, and $V_{Ga}3O_N$, are also donors. They are responsible for broad PL bands in the red-yellow part of the PL spectrum from GaN grown by ammonothermal method and containing high concentrations of the V_{Ga} , H, and O. Note that the isolated V_{Ga} and the $V_{Ga}O_N$ complex are likely nonradiative defects. 3,24,30

3.3 Shapes of PL bands

Shapes of PL bands in GaN are dictated by electron-phonon coupling and can be explained with a one-dimensional configuration-coordinate model.²⁰ The strength of electron-phonon coupling is described with the Huang-Rhys factor S (Table 1). For shallow acceptors (Mg_{Ga} and Be_{Ga}), S is small, and the PL band appears as a sharp peak (the ZPL) followed by decreasing in intensity LO phonon replicas. The Huang-Rhys factor increases with increasing acceptor ionization energy because the bound hole becomes more localized. For deep defects, broad PL bands are observed, and the ZPL is either weak or not observed because of the small weight of the ZPL in the band spectrum, $w_{ZPL} \approx \exp(-S)$.³¹ The shape of the band can often be simulated with Eq. (6). Examples for the C_N-related YL1 band and Be_{Ga}-related YL_{Be} band are shown in Fig. 3. The PL band shape, position of its maximum, fine structure if any, and capture coefficients represent fingerprints of the defect and are expected to be identical in different samples. Note, however, that local electric fields and other reasons sometimes cause significant broadening and shifts of PL bands.¹⁰ For some PL bands, the ZPL can be observed (the YL1 band has the ZPL at 2.59 eV), while for others, the magnitude of S is too large, and the ZPL cannot be found (the ZPL for the YL_{Be} band is expected at 3.2 eV with peak intensity about 10^{-12} from that of the band maximum).

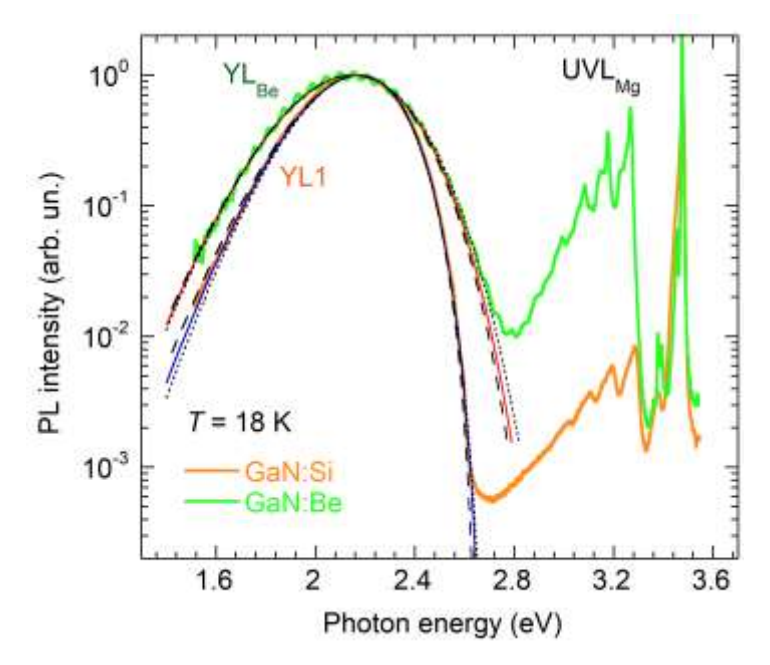


Figure 3. PL spectra Si-doped and Be-doped GaN at T=18 K. The solid, dotted, and dashed lines are calculated using Eq. (6) with the following parameters: $S_e=7.6$, 8.5, 6.5, $E_0^*=2.67$ eV, 2.69, 2.64 and $\hbar\omega_{max}=2.17$ eV for the YL1 band; $S_e=23$, 32, 19, $E_0^*=3.2$ eV, 3.4, 3.1 and $\hbar\omega_{max}=2.15$ eV for the YL_{Be} band.

Eq. (6) helps distinguish PL bands and reproduce their shapes. However, the fitting parameters may not be accurate or unique (Fig.3), especially if the exact location of the ZPL is unknown. In particular, similar PL band shapes can be obtained if parameters E_0^* and S_e in Eq. (6) are increased simultaneously. Figure 4 shows ranges of these parameters for which acceptable agreement with experimental data can be achieved. While for the YL1 band, the uncertainties in E_0^* and S_e are small, they are large for PL bands for which the ZPL is not observed. Table 1 shows the optimal values of E_0^* and S_e with their uncertainties.

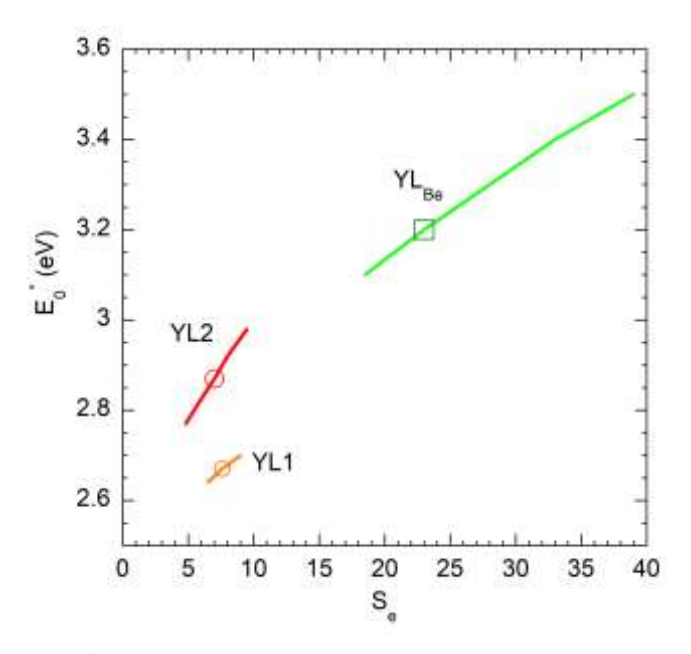


Figure 4. Ranges of parameters E_0^* and S in Eq. (6) providing acceptable fits for the shapes of the YL1, YL2, and YL_{Be} bands in GaN. Symbols show the optimal values.

Another critical parameter is the Franck-Condon shift d_{FC} . It is equal to the energy difference between the ZPL and band maximum. Since $\hbar \omega_{\text{max}}$ is known from the experiment, the uncertainty in the d_{FC} is similar to that of the E_0^* . Figure 5 shows the values of d_{FC} for selected defects in GaN.

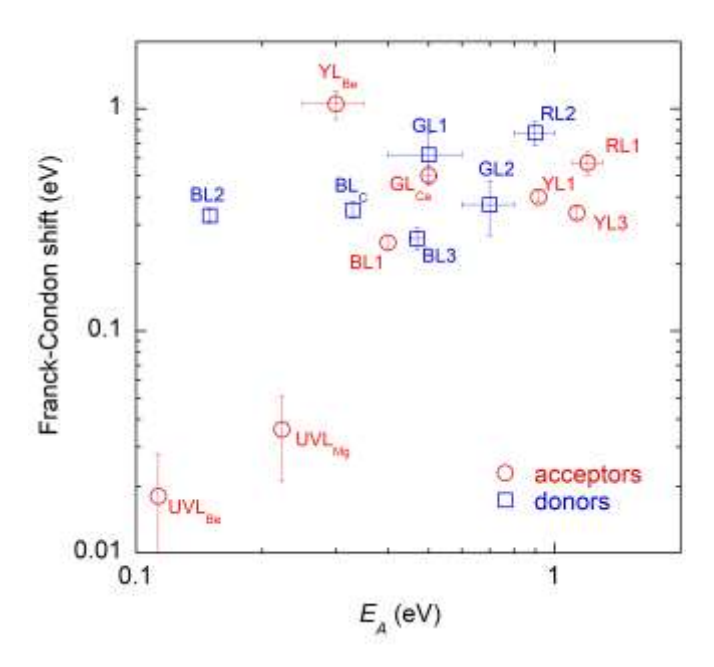


Figure 5. Franck-Condon shift as a function of the ionization energy for defects in GaN

3.4 Relation between photoluminescence intensity and defect concentration

It is commonly expected that PL intensity is proportional to the concentration of related defects. However, this is true only in limited cases and often leads to wrong conclusions. Furthermore, attempts to find the concentration of defects from PL are extremely rare. The problem of finding concentrations of defects is closely related to the problem of finding the absolute IQE. Both parameters can be reliably found for conductive n-type GaN samples from analysis of excitation intensity and temperature dependences and using rate equation models. ^{7,8,16,18,24,32} The concentration N can be found from the saturation of defect-related PL intensity (SSPL or TRPL) with increasing excitation intensity described with Eq. (7). ^{15,32} In this fit, the largest uncertainty originates from parameter η_0 - the absolute IQE in the limit of low excitation intensities. The η_0 can be found with high accuracy from the competition of recombination channels in samples where one of the PL bands is very strong, with the IQE approaching unity. ¹⁸ These samples can serve as standards of the IQE. The IQE from other samples can be estimated by comparison of integrated PL intensities with those in calibrated samples. The errors, in this case, may originate from different light extraction efficiencies in different samples. We conclude that the concentration N can be found with the accuracy of plus-minus half an order of magnitude. ³² Better accuracy can be achieved for relative concentrations of defects responsible for PL bands in the same sample. ^{23,32} For this, the hole-capture coefficients should be known. Indeed, the integrated PL intensities in n-type semiconductors at low excitation intensities and temperatures are proportional to the product of C_p and N.

Figure 6 shows the dependence of PL intensity on the concentration of the related defect for the Mg_{Ga}, Zn_{Ga}, and C_N defects responsible for the UVL, BL1, and YL1 bands, respectively, in GaN. The PL was measured in identical conditions, and the PL intensities are given in relative units, approximately equal to the IQE. For low concentrations ($N < 10^{16} \text{ cm}^{-3}$), the PL intensity increases linearly with N. For these samples, the N was found from the fit of the $\eta(P)$ dependences with Eq. (7). Such low concentrations of defects are challenging to detect with other techniques. For example, the typical detection limit in SIMS measurements for these impurities is about 10^{16} cm^{-3} (shown with a vertical dashed line). The quality of GaN samples analyzed in Fig. 6 is reasonably high (what can be concluded from a high intensity of the exciton emission), and the scatter of experimental points in the left half of this figure can be explained by different concentrations of nonradiative defects in different samples. For $N > 10^{16} \text{ cm}^{-3}$, the PL intensity cannot increase because the η is already close to unity. As a result, PL intensity becomes independent of N, and the scatter in the data can be attributed to different concentrations of nonradiative defects and/or to the effect of the surface.

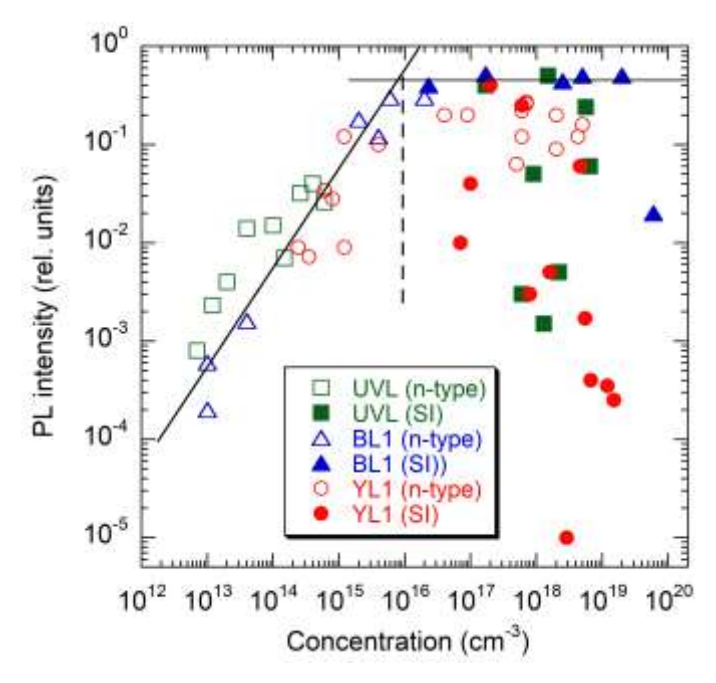


Figure 6. Dependence of PL intensity on the concentration of related defect. The UVL, BL1, and YL1 bands are related to the Mg_{Ga} , Zn_{Ga} , and C_N acceptors, respectively.

For semi-insulating GaN samples, no correlation between the PL intensity and N can be found (the filled symbols in Fig. 6). For $N > 10^{16}$ cm⁻³ (the N was found from SIMS measurements for most of these data points), only the Zn-related BL1 band remains very strong up to $N = 10^{19}$ cm⁻³, whereas PL bands related to C and Mg are often very weak in SI samples. This may happen because there are no equilibrium charge carriers in SI samples, and the dynamics of recombination of photogenerated carriers are often complex. Among the unusual effects in such samples is the abrupt and tunable quenching of PL, briefly analyzed below.

3.5 Quenching of photoluminescence

The intensity of defect-related PL decreases exponentially with increasing temperature above a characteristic temperature T_0 , a process called PL quenching. In most cases, the temperature dependence can be described with Eq. (4), yet the meaning of parameters C and E_A depends on the quenching mechanism.³³ PL from defects in conductive n-type GaN is quenched with the Schön-Klasens mechanism).^{34,35} According to this mechanism, bound holes are thermally emitted to the valence band and re-captured by nonradiative defects. The E_A in Eq. (4) is the ionization energy (the distance from the charge transition level to the VBM plus a barrier for the hole capture/emission, if any). The parameter C is proportional to the PL lifetime and the hole-capture coefficient: $C = (1 - \eta_0) \tau_0 C_p N_v g^{-1}$. The critical temperature of the quenching, $T_0 = E_A(k \ln C)^{-1}$, can be viewed as the temperature at which the characteristic time of thermal emission of holes to the valence band becomes equal to the PL lifetime.¹¹ An example of the quenching of the C_N -related YL1 band by the Schön-Klasens mechanism in conductive n-type GaN is shown in Fig. 7 and fitted with Eq. (4) (the solid line 1). In this mechanism, T_0 is independent of the excitation intensity (T_0 =445 K for n-type GaN in Fig. 7) unless P_{exc} is very high and PL saturates. The T_0 increases with the concentration of free electrons (through a parameter τ_0) and increases in samples with the IQE close to unity. ^{18,33}

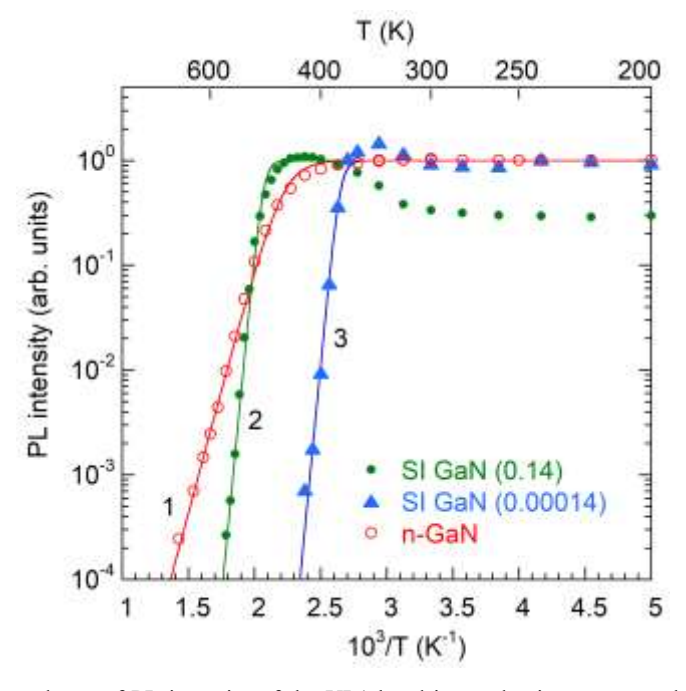


Figure 7. Temperature dependence of PL intensity of the YL1 band in conductive *n*-type and SI GaN samples. P_{exc} (in W/cm²) is indicated in parentheses. The solid lines are the fits using Eq. (4) with the following parameters: $E_A = 0.84$ eV, $C_p = 3 \times 10^{-7}$ cm³/s, and $\tau_0 = 0.5$ ms (curve 1); $E_A = 2.6$ eV and $C = 1 \times 10^{27}$ (curve 2); $E_A = 2.6$ eV and $C = 5 \times 10^{34}$ (curve 3).

In high-resistivity or semi-insulating GaN, PL is usually quenched by the abrupt and tunable mechanism.⁷ Examples include the C_N -related YL1 band,³⁶ Zn-related BL1 band,⁷ Mg-related UVL band,³⁷ Be-related YL_{Be} and UVL_{Be} bands,²⁷ Ca-related GL_{Ca} band,²³ V_N-related GL2 band,²⁰ and the BL2 band caused by the C_NH_i complex.¹² Figure 7 shows the $I^{PL}(T)$ dependences for the YL1 band in semi-insulating GaN:C. The quenching is abrupt (" E_A " = 2.6 eV) and tunable by excitation intensity: the I_0 increases from 375 to 475 K as the I_0 increases from 1.4×10⁻⁴ to 0.14 W/cm² (curves 2 and 3 in Fig. 7). Note that the slope of the quenching has no physical meaning. It is an abrupt transition from the conditions

when PL intensities are dictated by the capture of holes to the conditions when electron-hole recombination predominantly occurs via defects that capture electrons fast.

In the classical case of abrupt and tunable quenching,⁷ dominant nonradiative deep donors become saturated with photogenerated holes at $T < T_0$. This also causes the accumulation of photogenerated electrons in the conduction band, population inversion, and the conversion of p-type conductivity to n-type.³⁸ In such conditions, the IQE of PL via acceptors is very high. With increasing temperature, at $T = T_0$, the thermal emission of holes from the radiative acceptor unblocks the dominant nonradiative channel. This occurs when the concentration of holes in the valence band, which are thermally emitted from the acceptor, becomes equal to the concentration of optically generated holes. Since the latter is proportional to the excitation intensity or electron-hole generation rate G, the T_0 increases with P_{exc} or G. The actual ionization energy of the acceptor (E_A) in this case can be found from the $T_0(G)$ dependence (Eq. (5)).

For both mechanisms, T_0 is proportional to E_A ; compare Eqs. (3) and (5). The slope of the $T_0(E_A)$ dependence is the same when B/G = C, or $(N_A - N_D)/(\eta_0 G) = \tau_0$. For typical parameters, this occurs when P_{exc} is of the order of 0.1 W/cm² (a typical excitation power density of an unfocused beam of a HeCd laser). Figure 8 shows the dependence of T_0 on E_A for major defects in undoped GaN and GaN doped with C, Mg, or Zn. The dashed lines indicate the typical range of parameter C (between 10^7 and 10^{10}). Note that the data points obtained from the abrupt and tunable quenching in semiinsulating GaN samples (the filled symbols for the BL1 and YL1 bands) are also within this range. A few data points for the BL1 band outside the outlined region correspond to GaN:Si, Zn samples with an unusually high concentration of electrons (~10¹⁹ cm⁻³) and extraordinarily high IQE (0.8-0.95). By using this dependence, we can predict the ionization energy of defects in GaN from observation of To in the temperature dependence of PL intensity or PL lifetime. Sometimes this approach gives more realistic results than the E_A found by fitting the slope of the $I^{PL}(T)$ dependence. For example, the values of E_A between 0.06 and 2.6 eV can be obtained for the YL1 band from the slope of the $I^{PL}(T)$ dependence. 36,38 However, the YL1 quenching begins between 450 and 550 K in all these samples, which indicates that $E_A \approx 0.8$ eV. Another example is the Be_{Ga}-related yellow band. In Be-doped GaN layers grown by MBE or MOCVD (semi-insulating and conductive n-type), the quenching of the YL_{Be} band begins at 180-200 K, in agreement with the estimated $E_A = 0.30$ eV for the Be_{Ga} defect.³⁹ A similar yellow band in bulk GaN with high concentrations of Be and O is attributed to the Be_{Ga}O_N complex.⁴⁰ This yellow band is quenched only at T > 500 K,⁴¹ which indicates that the related defect level is located at about 0.8 eV above the VBM.

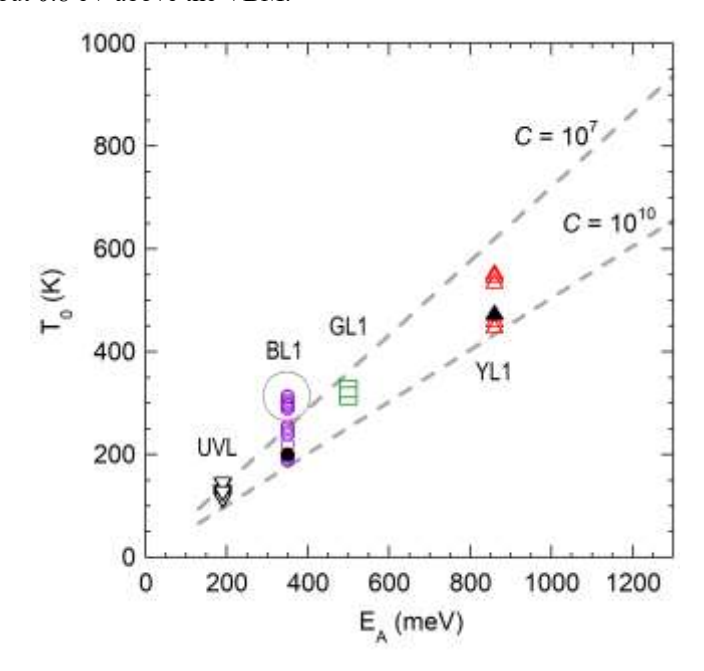


Figure 8. Dependence of critical temperature of PL quenching on the acceptor ionization energy for the UVL, BL1, GL1, and YL1 bands in GaN. Empty symbols are data from conductive *n*-type samples, and the filled black symbols are for semi-insulating samples exhibiting the abrupt and tunable quenching ($P_{exc} \approx 0.1 \text{ W/cm}^2$). The circled data points for the BL1 band are from samples with exceptionally high η_0 and small τ_0 .

The third mechanism of PL quenching is the Seitz-Mott mechanism.^{42,43} The PL quenching is caused by a gradual replacement of radiative transitions with non-radiative ones in the same defect.³⁸ In this mechanism, E_A is the energy difference between the potential minimum of the excited state and the cross-over point of the excited and ground states of the defect, and C is the product of PL lifetime in the excited state and the vibrational frequency of the defect. This mechanism of PL quenching is commonly used to explain PL from F centers in alkali halides.^{44,45} However, we cannot find any defect in GaN, the PL from which is quenched by this mechanism. Earlier, we proposed that the Seitz-Mott mechanism can explain the quenching of the GL2 and RL2 bands with $E_A \approx 0.1$ eV. However, the accumulated in the last 15 years' experimental data indicate that the quenching of these PL bands is rather caused by the thermal emission of electrons from excited states of deep donors to the conduction band.^{8,20,28}

PL intensity from defects sometimes increases with temperature, the phenomenon often called the "negative thermal quenching" (NTQ), with many examples in GaN. These $I^{PL}(T)$ dependences can be explained with rate equation models. The typical reason for the NTQ is the quenching of another PL band or a nonradiative recombination channel and associated with this redistribution of charge carrier flows.³³

3.6 Parameters of defects

From the analysis of temperature dependences of PL intensity or PL lifetime in n-type GaN, the hole-capture coefficient C_p can be found (see Eqs. (2) and (4)). Alternatively, the C_p can be estimated by comparing integrated PL intensities because the PL intensity at low temperatures is proportional to C_pN . The results for defects in GaN are summarized in Table 1 and Fig. 9(a). For acceptors, C_p is between 10^{-7} and 10^{-6} cm³/s. It is possible that acceptors with smaller C_p exist but cannot be found in the PL spectrum because of relatively high concentrations of typical contaminants, such as Mg, C, or Zn. The C_p for the RY3 defect is exceptionally high because holes are captured by a shallow effective-mass state near the VBM.²² Donors capture holes less efficiently because they are neutral. The data for the GL1, BL2, and BL3 bands look reasonable. The very low value of C_p for the BL_C band, obtained from the comparison of PL intensities,⁵ is surprising.

Note that C_p may have a strong temperature dependence if a hole capture is a thermally activated process.⁴⁶ For example, the C_p for the C_N acceptor is predicted to increase by two orders of magnitude as the temperature increases from ~50 to 600 K.⁴⁷ This dependence is attributed to the expected barrier for the hole capture. However, in the experiment, no variation of the C_p for the YL1 band could be found for temperatures between 18 and 500 K.³ It appears that there are no substantial barriers for the hole capture at acceptors commonly contributing to PL in GaN. It is possible that PL bands from defects with significant barriers for hole capture are not observed because they are extremely weak.

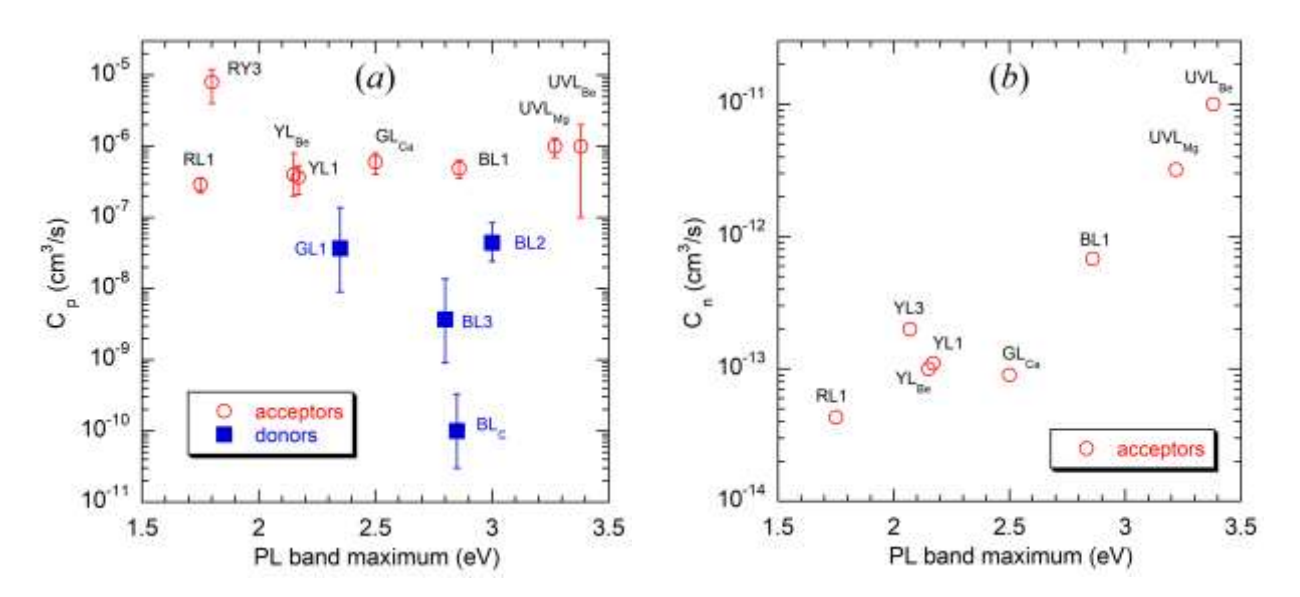


Figure 9. Parameters of defects in GaN. (a) Hole-capture coefficient (b) Electron-capture coefficient.

The electron-capture coefficient C_n can be found for acceptors in conductive n-type GaN from TRPL (Eq. (1)). As can be seen from Fig. 9b and Table 1, the C_n increases from 10^{-13} cm³/s for deep acceptors to 10^{-11} cm³/s for shallow ones. These are typical values for radiative transitions and they reasonably agree with predictions from first-principles calculations.⁴⁸ For donors, C_n cannot be found from TRPL because electrons are captured fast (nonradiatively) at excited states, and the PL lifetime is independent of the C_n .

3.7 Comparison with first-principles calculations

Early first-principles calculations for defects in semiconductors relied on local or semi-local approximations to the density functional theory (DFT). Since these calculations significantly underestimated the calculated bandgap, various correction methods were developed. As it became known later, the calculated parameters of defects in GaN (such as ZPL and position of PL band maximum) were not accurate, especially for multi-charged defects. For example, the C_N was predicted to be a shallow acceptor with $E_A \approx 0.2$ eV, and the 3–/2– level of the V_{Ga} was calculated at 1.1 eV.⁴⁹ These inaccurate predictions contributed to wrong identifications of PL bands in GaN. In particular, the YL band with a maximum at 2.2 eV in undoped GaN was often attributed to the V_{Ga} or $V_{Ga}O_N$ defects, which contradicts the modern view.³

Currently, the most common approach for the theoretical analysis of defects is the hybrid DFT, and the most popular hybrid functional used in this field is the Heyd-Scuseria-Ernzerhof (HSE) functional. Several versions of hybrid functionals are used to describe defects in GaN, and the results of the calculations are slightly different. Figure 10 compares experimentally found positions of PL band maxima with those calculated by three groups – D. Demchenko (DD), 20,12,27,23,11,39 Van de Walle (VDW), 14,53 and Lany and Zunger (LZ). A good agreement with the experiment has been achieved for the C_N defect. For many defects, the PL maximum is predicted at lower photon energy than observed in the experiment.

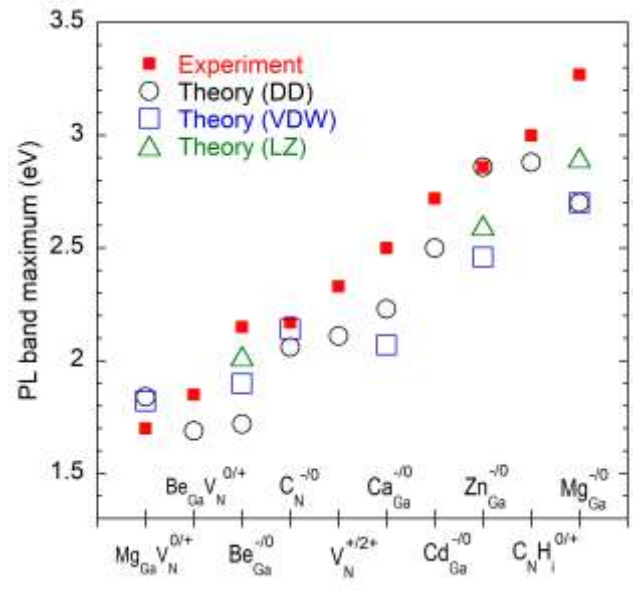


Figure 10. Positions of PL band maxima for defects in GaN compared with first-principles calculations.

Several puzzles in PL from defects in GaN remain unsolved. One is the dual nature of acceptors, a coexistence of a deep state with a localized hole and a shallow state with a delocalized hole, predicted by theory. ⁵⁴ In particular, the UVL_{Mg} band was attributed to the shallow state of the Mg_{Ga} defect, and the blue luminescence (BL_{Mg}) band in GaN heavily doped with Mg was thought to be caused by the deep state. However, analysis of experimental results indicates that only the UVL_{Mg} band with a maximum at 3.28 eV is related to the isolated Mg_{Ga} defect, whereas the BL_{Mg} band with a maximum at 2.7-2.9 eV is caused by transitions from a deep donor to the shallow Mg_{Ga} acceptor. ^{1,11} Another dual-nature acceptor in GaN is the Be_{Ga} defect. ⁵⁴ Recent experimental results indicate that the yellow band (YL_{Be}) with a maximum at 2.15 eV in Be-doped GaN is caused by electron transitions via the deep state of the Be_{Ga} acceptor, ³⁹ in agreement with

theoretical predictions. 14,54 The UVL_{Be} band with a maximum at 3.38 eV has been attributed to the shallow state of the Be_{Ga} acceptor. 55 However, it is not clear why there is no correlation between the UVL_{Be} and YL_{Be} bands.

4. SUMMARY

Identifying defects in GaN and understanding their properties are needed to eliminate defects or reduce their detrimental effect on devices. PL is one of the most powerful tools for studying point defects in GaN. The classification of PL band shapes, positions, and other properties allows us to recognize defects in PL spectra. The shapes of PL bands from defects in GaN can be explained using a one-dimensional configuration coordinate model. Important parameters have been determined for several defects, such as the ZPL, phonon energies, Huang-Rhys factor, electron- and hole-capture coefficients. These parameters help develop theoretical approaches to describe and predict the defect properties with high precision. GaN serves as the case study, and PL from defects in GaN provides the most reliable experimental data for this purpose.

ACKNOWLEDGMENTS

This work was supported by the National Science Foundation (grant DMR-1904861).

REFERENCES

[1] Reshchikov, M. R. and Morkoç, H., "Luminescence properties of defects in GaN", J. Appl. Phys. 97, 061301 (2005).

- [5] Reshchikov, M. A., Vorobiov, M., Demchenko, D. O., Özgür, Ü., Morkoç, H., Lesnik, A., Hoffmann, M. P., Hörich, F., Dadgar, A. and Strittmatter, A., "Two charge states of the C_N acceptor in GaN: Evidence from photoluminescence", Phys. Rev. B 98, 125207 (2018).
- [6] Reshchikov, M. A., "Fine Structure of the Carbon-Related Blue Luminescence Band in GaN", Solids **3**, 231-236 (2022).
- [7] Reshchikov, M. A., Kvasov, A. A., Bishop, M. F., McMullen, T., Usikov, A., Soukhoveev, V. and Dmitriev, V. A., "Tunable and abrupt thermal quenching of photoluminescence in high-resistivity Zn-doped GaN", Phys. Rev. B **84**, 075212 (2011).
- [8] Reshchikov, M. A., "Measurement and analysis of photoluminescence in GaN", J. Appl. Phys. **129**, 121101 (2021).
- [9] Reshchikov, M. A., Olsen, A. J., Bishop, M. F. and McMullen, T., "Superlinear increase of photoluminescence with excitation intensity in Zn-doped GaN", Phys. Rev. B. 88, 075204 (2013).
- [10] Reshchikov, M. A., "Giant shifts of photoluminescence bands in GaN", J. Appl. Phys. 127, 055701 (2020).
- [11] Reshchikov, M. A., Ghimire, P. and Demchenko, D. O., "Magnesium acceptor in gallium nitride: I. Photoluminescence from Mg-doped GaN", Phys. Rev. B **97**, 205204 (2018).
- [12] Reshchikov, M. A., Andrieiev, O., Vorobiov, M., McEwen, B. Shahedipour-Sandvik, F., Ye, D. and Demchenko, D. O., "Stability of the C_NH_i complex and the BL2 luminescence band in GaN", Phys. Stat. Sol. (b) **258**, 2100392 (2021).
- [13] Alkauskas, A., McCluskey, M. D. and Van de Walle, C. G., "Tutorial: Defects in semiconductors Combining experiment and theory", J. Appl. Phys. 119, 181101 (2016).
- [14] Lyons, J. L., Wickramaratne, D. and Van de Walle, C. G., "A first-principles understanding of point defects and impurities in GaN". J. Appl. Phys. **129**, 111101 (2021).
- [15] Reshchikov, M. A., "Time-resolved photoluminescence from defects in GaN", J. Appl. Phys. 115, 103503 (2014).

^[2] Lyons, J. L., Janotti, A. and Van de Walle, C. G., "Carbon impurities and the yellow luminescence in GaN", Appl. Phys. Lett. **97**, 152108 (2010).

^[3] Reshchikov, M. A., "On the Origin of the Yellow Luminescence Band in GaN", Phys. Stat. Sol. (b) 2200488 (2022).

^[4] Reshchikov, M. A., McNamara, J. D., Zhang, F., Monavarian, M., Usikov, A., Helava, H., Makarov, Yu. and Morkoç, H., "Zero-phonon line and fine structure of the yellow luminescence band in GaN", Phys. Rev. B **94**, 035201 (2016).

- [16] Reshchikov, M. A., Internal Quantum Efficiency of Photoluminescence in Wide-Bandgap Semiconductors, Chapter in Photoluminescence: Applications, Types and Efficacy, Ed. M. A. Case and B. C. Stout, Nova Science Publishers, Inc., New York, pp. 53-120 (2012).
- [17] Muth, J. F., Lee, J. H., Shmagin, I. K., Kolbas, R. M., Casey, H. C., Jr., Keller, B. P., Mishra, U. K. and DenBaars, S. P., "Absorption coefficient, energy gap, exciton binding energy, and recombination lifetime of GaN obtained from transmission measurements", Appl. Phys. Lett. 71, 2572 (1997).
- [18] Reshchikov, M. A., Foussekis, M. A., McNamara, J. D., Behrends, A., Bakin, A. and Waag, A., "Determination of the absolute internal quantum efficiency of photoluminescence in GaN co-doped with Zn and Si", J. Appl. Phys. 111, 073106 (2012).
- [19] Reshchikov, M. A., "Temperature dependence of defect-related photoluminescence in III-V and II-VI semiconductors", J. Appl. Phys. 115, 012010 (2014).
- [20] Reshchikov, M. A., Demchenko, D. O., McNamara, J. D., Fernández-Garrido, S. and Calarco, R., "Green luminescence in Mg-doped GaN", Phys. Rev. B **90**, 035207 (2014).
- [21] Reshchikov, M. A., McNamara, J. D., Toporkov, M., Avrutin, V., Morkoç, H., Usikov, A., Helava, H. and Makarov, Yu., "Determination of the electron-capture coefficients and the concentration of free electrons in GaN from photoluminescence", Sci. Rep. 6, 37511 (2016).
- [22] Reshchikov, M. A., Sayeed, R. M., Özgür, Ü., Demchenko, D. O., McNamara, J. D., Prozheeva, V., Tuomisto, F., Helava, H., Usikov, A. and Makarov, Yu., "Unusual properties of the RY3 center in GaN", Phys. Rev. B 100, 045204 (2019).
- [23] Reshchikov, M. A., Demchenko, D. O., Vorobiov, M., Andrieiev, O., McEwen, B., Shahedipour-Sandvik, F., Sierakowski, K., Jaroszynski, P. and Bockowski M., "Photoluminescence related to Ca in GaN", Phys. Rev. B 106, 035206 (2022).
- [24] Reshchikov, M. A., Demchenko, D. O., Ye, D., Andrieiev, O., Vorobiov, M., Grabianska, K., Zajac, M., Nita, P., Iwinska, M., Bockowski, M., McEwen, B. and Shahedipour-Sandvik, F., "The effect of annealing on photoluminescence from defects in ammonothermal GaN", J. Appl. Phys. 131, 035704 (2022).
- [25] Thomas, D. G., Hoppfield, J. J. and Augustyniak, W. M., "Kinetics of Radiative Recombination at Randomly Distributed Donors and Acceptors", Phys. Rev. 140, A202-220 (1965).
- [26] Korotkov, R. Y., Reshchikov, M. A. and Wessels, B. W., "Acceptors in undoped GaN studied by transient photoluminescence", Physica B **325**, 1-7 (2003).
- [27] Vorobiov, M., Andrieiev, O., Demchenko, D. O. and Reshchikov, M. A., "Point Defects in Beryllium Doped GaN", Phys. Rev B **104**, 245203 (2021).
- [28] Vorobiov, M., Andrieiev, O., Demchenko, D. O. and Reshchikov, M. A., unpublished.
- [29] Lyons, J. L., Alkauskas, A., Janotti, A. and Van de Walle, C. G., "First-principles theory of acceptors in nitride semiconductors," Phys. Stat. Sol. (b) **252**, 900–908 (2015).
- [30] Reshchikov, M. A., "Photoluminescence from Vacancy-Containing Defects in GaN", Phys. Stat. Sol. (a) 2200402 (2022).
- [31] Alkauskas, A., Buckley, B. B., Awschalom, D. D. and Van de Walle, C. G., "First-principles theory of the luminescence lineshape for the triplet transition in diamond NV centers", New J. Phys. 16, 073026 (2014).
- [32] Reshchikov, M. A., Usikov, A., Helava, H., Makarov, Yu., Prozheeva, V., Makkonen, I., Tuomisto, F., Leach, J. H. and Udwary, K., "Evaluation of the concentration of point defects in GaN", Sci. Rep. 7, 9297 (2017).
- [33] Reshchikov, M. A., "Mechanisms of thermal quenching of defect-related luminescence in semiconductors", Phys. Stat. Sol. A **218**, 2000101 (2020).
- [34] Schön, M., "Zum Leuchtmechanismus der Kristallphosphore", Z. Phys. 119, 463-471 (1942).
- [35] Klasens, H. A., "Transfer of energy between centers in zinc sulphide phosphors", Nature 158, 306-307 (1946).
- [36] Reshchikov, M. A., Albarakati, N. M., Monavarian, M., Avrutin, V. and Morkoç, H., "Thermal quenching of the yellow luminescence in GaN", J Appl. Phys. 123, 161520 (2018).
- [37] Reshchikov, M. A., McNamara, J., Fernandez, S. and Calarco, R., "Tunable thermal quenching of photoluminescence in Mg-doped p-type GaN", Phys. Rev. B 87, 115205 (2013).
- [38] Reshchikov, M. A., "Temperature dependence of photoconductivity in Zn-doped GaN", AIP Conf. Proc. 1583, 292-296 (2014).
- [39] Reshchikov, M. A., Vorobiov, M., Andrieiev, O., McEwen, B., Rocco, E., Meyers, V., Demchenko, D. O. and Shahedipour-Sandvik, F., "Photoluminescence from Be-Doped GaN Grown by Metal-Organic Chemical Vapor Deposition", Phys. Stat. Sol. (b) 202200487 (2022).

- [40] Teisseyre, H., Lyons, J. L., Kaminska, A., Jankowski, D., Jarosz, D., Bockowski, M., Suchocki, A. and Van de Walle, C. G., "Identification of yellow luminescence centers in Be-doped GaN through pressure-dependent studies", J. Phys. D: Appl. Phys. **50**, 22LT03 (2017).
- [41] Lamprecht, M., Thonke, K., Teisseyre, H. and Bockowski, M., "Extremely Slow Decay of Yellow Luminescence in Be-Doped GaN and Its Identification", Phys. Stat. Sol. (b) 255, 1800126 (2018).
- [42] Seitz, F., "An interpretation of crystal luminescence", Trans. Faraday Soc. 35, 74-85 (1939).
- [43] Gurney R. W. and Mott, N. F., "Luminescence in solids", Trans. Faraday Soc. 35, 69-73 (1939).
- [44] G. Baldacchini, "Radiative and nonradiative processes in color crystals", in *Advances in Nonradiative Processes in Solids*, Ed. B. Di Bartolo, Plenum Press, New York, 219-259 (1991).
- [45] Stoneham, A. M., Theory of Defects in Solids, Clarendon Press, Oxford, 555-698 (1975).
- [46] Alkauskas, A., Yan, Q. and Van de Walle, C. G. "First-principles theory of nonradiative carrier capture via multiphonon emission", Phys. Rev. B **90**, 075202 (2014).
- [47] Wickramaratne, D., Dreyer, C. E., Monserrat, B., Shen, J.-X., Lyons, J. L., Alkauskas, A. and Van de Walle, C. G., "Defect identification based on first-principles calculations for deep level transient spectroscopy", Appl. Phys. Lett. 113, 192106 (2018).
- [48] Dreyer, C. E., Alkauskas, A., Lyons, J. L. and Van de Walle, C. G., "Radiative capture rates at deep defects from electronic structure calculations", Phys. Rev. B **102**, 085305 (2020).
- [49] Van de Walle, C. G. and Neugebauer, J., "First-principles calculations for defects and impurities: Applications to III-nitrides", J. Appl. Phys. **95**, 3951-3879 (2004).
- [50] Heyd, J., Scuseria, G. E. and Ernzerhof, M., "Hybrid functionals based on a screened Coulomb potential", J. Chem. Phys. 118, 8207-8215 (2003).
- [51] Demchenko, D. O. and Reshchikov, M. A., "Koopmans' tuning of HSE hybrid density functional for calculations of defects in semiconductors: A case study of carbon acceptor in GaN, J. Appl. Phys. **127**, 155701 (2020).
- [52] Reshchikov M. A., and Demchenko, D. O., "Roadmap for Point Defects in GaN", a chapter in *Semiconductors* and *Semimetals*, edited by Zetian Mi and Hark Hoe Tan, Vol. 111, pp. 133-152 (2022).
- [53] Lyons, J. L., Janotti, A. and Van de Walle, C. G., "Impact of Group-II Acceptors on the Electrical and Optical Properties of GaN", Jap. J. Appl. Phys. **52**, 08JJ04 (2013).
- [54] Lany, S. and Zunger, A., "Dual nature of acceptors in GaN and ZnO: The curious case of the shallow Mg_{Ga} deep state", Appl. Phys. Lett. **96**, 142114 (2010).
- [55] Demchenko, D. O., Vorobiov, M., Andrieiev, O., Myers, T. H. and Reshchikov, M. A., "Shallow and deep states of beryllium acceptor in GaN: Why photoluminescence experiments do not reveal small polarons for defects in semiconductors", Phys. Rev. Lett. **126**, 027401 (2021).